EXPERIMENTAL AND ANALYTICAL STUDY OF A SELF-REGULATED FLOW CONTROL DEVICE DEVELOPED FOR DYNAMIC COLD-PLATES TO COOL HIGH-POWER DENSITY MULTI-CHIP MODULES

by

RISHI RUBEN PALANIKUMAR

Presented to the Faculty of the Graduate School of

The University of Texas at Arlington in Partial Fulfillment

of the Requirements

for the Degree of

MASTER OF SCIENCE IN MECHANICAL ENGINEERING

THE UNIVERSITY OF TEXAS AT ARLINGTON

May 2018

Acknowledgements

I would like to express deep gratitude to my supervising professor Dr. Dereje Agonafer for his encouragement, support, and guidance during the course of my research at The University of Texas at Arlington. He gave me the opportunity to work on industry-funded projects and attend conferences which provided me with great insight into modern industrial trends.

I would like to sincerely thank Dr. Haji-Sheikh and Dr. Andrey Beyle for being on my thesis committee and for their valuable comments on my work. Special thanks to Rajesh Kasukurthy for his invaluable guidance and mentorship. I am also thankful to Pavan Rajmane for helping me out with the thermal chamber, my teammate Barath Ragul and all other EMNSPC team members for their support during my research work.

I am very much obliged to Ms. Wendy Lee Ryan for assisting me with administrative work. I would also like to thank the Mechanical engineering department faculty and staff who have supported me throughout my graduate studies.

I would like to thank my parents, Mr. B. Palanikumar and Mrs. P. Kavitha who have served as motivation and inspiration throughout my life. Last but not least, I would like to thank Swetha Karthikeyan Muralidaran and all my friends without whose emotional support none of this would have been possible.

April 27, 2018

Abstract

EXPERIMENTAL AND ANALYTICAL STUDY OF A SELF-REGULATED FLOW CONTROL DEVICE DEVELOPED FOR DYNAMIC COLD-PLATES TO COOL HIGH-POWER DENSITY MULTI-CHIP MODULES

Rishi Ruben Palanikumar, MS

The University of Texas at Arlington, 2018

Supervising Professor: Dereje Agonafer

Modern high-power density modules often demand high amounts of power be invested in their cooling processes. Uneven heating at the chip level creates hotspots and temperature gradients across the module. A very effective way to conserve pumping power and address hotspots on the module is by targeted delivery of liquid coolant. One way to enable such targeted delivery of coolant is by using dynamic cold-plates (DCP) coupled with self-regulated flow control devices. This paper deals with the optimization and characterization of one such flow control device (FCD). The self-regulated FCD is actuated by a heat reactive shape memory alloy, Nitinol. A novel dual spring coupling comprised of a helical Nitinol spring and a Stainless-steel tension spring is used to regulate fluid flow as a function of temperature. Extensive experimental testing was done on Nitinol springs to estimate the amount of force generated and displacement produced during its phase change. Nitinol hysteresis was also comprehensively documented after experimental testing. The prototype FCD that would house the dual spring actuator was

designed to deliver a range of flowrates, highest of which can sufficiently cool a 200W module with heat density of 50W/cm2. 6Sigma is used to do CFD analysis on the flow control device. An experimental test rig was built to test the FCD prototype. Flow range over a fixed temperature range was obtained using the same.

TABLE OF CONTENTS

List of Illustrations

List of Tables

List of Graphs

Chapter 1

DYNAMIC COLD PLATES

Modern high-power density modules demand highly efficient cooling solutions be employed in data-centers to ensure economic feasibility. Multi-chip modules give rise to non-uniform temperature distribution across the die. This is primarily due to varying power densities observed amongst the different functional units on the die. Localized regions of high temperature known as ‘hot spots’ are observed on different localized regions of the module, owing to the non-uniform temperature distribution [1]. These hot spots result in large temperature gradients across the die, which can negatively impact reliability and performance of the module. Conventional cold-plates must be operated to cool the highest temperature regions of the module, resulting in more coolant than what is actually required being used to sufficiently cool individual regions of the module. One way to address non-uniform power distribution at the chip level is by using a dynamic cold-plate. A dynamic cold plate (DCP), unlike a conventional cold-plate has several sections with individual inlets and outlets for each section. This allows for targeted delivery of liquid coolant between different sections of the DCP. To provide targeted delivery of liquid coolant, a control system to sense junction temperature is required. Based on temperatures at different regions of the module, different amounts of coolant are supplied to each section of the DCP.

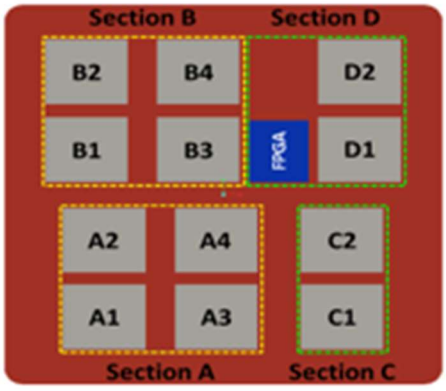

Figure 1-1 Multi-chip module with several functional units [2].

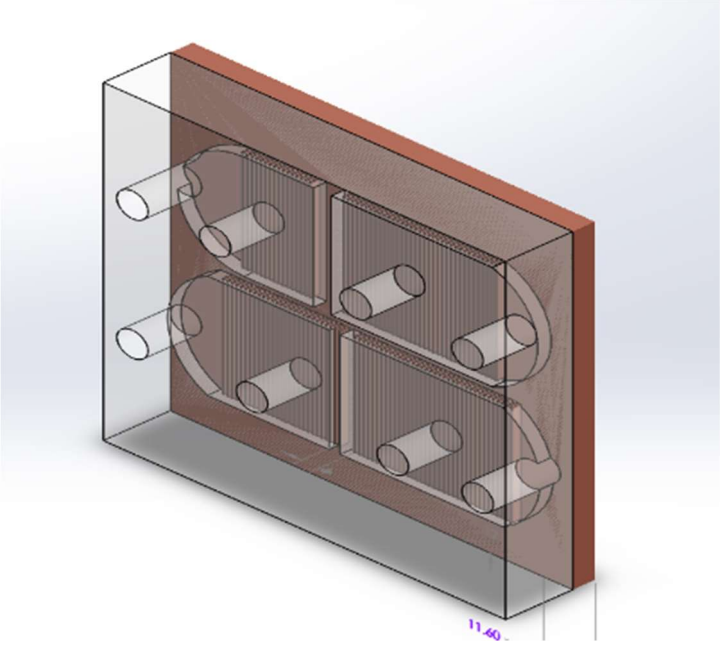

Figure 1-2 Dynamic cold plate 3D model [2].

Previous work on a DCP designed with four sections to cool a multi-chip module was done by Kunal Atulkumar Shah [2]. Each DCP section had coolant delivered by a dedicated pump. This meant that the DCP used four pumps, one for each section of the DCP. All four pumps were operated based on feedback from temperature sensors that read temperatures of different regions of the multi-chip module. Suitable control systems were used to control fluid delivery by the pumps. The literature claims a 28.32% reduction in pumping power requirement was observed while using a DCP when compared to a traditional cold-plate [2].

Chapter 2

FLOW CONTROL DEVICE

2.1. Purpose of a flow control device

This thesis deals with the concept of using a temperature sensing flow control device to further improve efficiency of a DCP. Self-regulated flow control devices (FCDs) when attached to the outlets of DCP sections, can vary flow rate as a function of temperature of the coolant (water) flowing through each one of them. This allows for sections of the DCP at high temperatures to receive more coolant as compared to cooler sections of the DCP. An array of FCDs essentially distribute flow between each other, thereby negating the need for individual pumps for each DCP section.

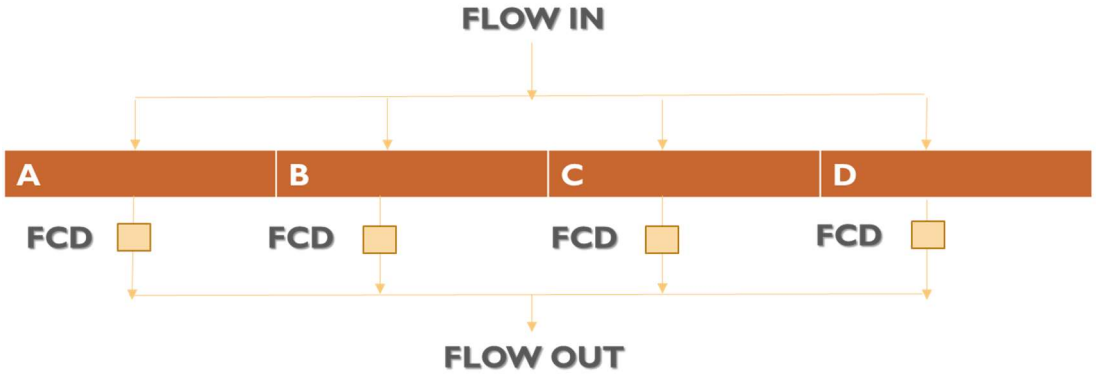

Figure 2-1 Schematic of a DCP coupled with FCDs (A, B, C, D represent four sections of the DCP)

In a scenario where all DCP sections require maximum flowrates (100% utilization), the FCDs would provide least resistance to coolant flow and the pressure across the DCP would be minimum. If this value of pressure difference across the DCP at 100% utilization is perpetually maintained across the DCP for all utilizations by reducing flow delivery from the pump, significant savings in pumping power can be made. It is also to be noted that the use of an array of FCDs allows for centralized pumping rather than having individual pumps for each section.

As seen from Manasa's work [3] it is clear to see that centralized pumping can provide significant reduction in pumping power when compared to distributed pumps.

2.2. FCD material selection

The actuator used in the FCD must be capable of reacting to change in coolant (water) temperature. The actuator material is also constantly in contact with water and hence must be resistant to corrosion. Deflection produced per unit rise in temperature and repeatability over several cycles of use are the highest priorities during material selection for the FCD. Several other factors exclusive to the FCD use-case were also considered during material selection. The material of choice after comparing numerous materials based on several criteria is Nitinol shape memory alloy. The table validates Nitinol over the various criteria that were considered during material selection.

Table 2-1 Nitinol material properties [4]

YOUNG'S MODULUS	Austenite	approx. 83 GPa
	Martensite	approx. 28 to 41 GPa
YIELD STRENGTH	Austenite	195 to 690 MPa
	Martensite	70 to 140 MPa
ULTIMATE TENSILE STRENGTH		895 MPa

Table 2-2 FCD Actuator material selection

Selection criteria	Comments
Composition of the material	Niti
Deflection	Very good
Cost	Average
Corrosion	Very good
Energy consumed for deflection	Exceptional
Relaxation time	Good
Repeatability of n number of cycles	Exceptional
Ease of developing and availability in market	Very good
Flexibility in operation as per aging and changing need	Good
Can thermal gradient within the pipe create issues	Good
Effect of cooling and heating hysteresis curve on performance	Can be minimized in several ways
Can it be used passively for given application	Yes

Nitinol is a shape memory alloy that reacts to application of heat with a change in its shape. Nitinol has two phases, a low temperature martensite phase and a high temperature austenite phase. Nitinol undergoes a phase change from martensite to austenite on heating accompanied by an increase in its young's modulus and shear modulus. This implies that in its high temperature austenite phase, nitinol is much stiffer compared to its low temperature martensite phase, in which it can more readily be deformed.

Nitinol phase change does not occur at fixed temperatures. Rather, the phase change occurs over a range of temperature. Nitinol also exhibits a difference in the transformation temperatures upon heating from martensite to austenite and cooling from austenite to martensite. This difference results in a lag during the cooling cycle. This lag between the

heating and cooling cycles is called thermal hysteresis. Several alloying methods can be employed to manipulate the hysteresis of Nitinol and ensure that the lag is acceptably small.

2.2.1. Two-way Nitinol

Two-way Nitinol can remember two different shapes: one at low temperatures, and one at the high-temperature [5]. This means that nitinol has fixed shapes for 100% Martensite and 100% Austenite compositions. Two-way nitinol can freely transform between its high temperature and low temperature phases purely by thermal loading and unloading. A two-way nitinol helical spring was experimentally tested by thermal cycling in a thermal chamber. The plot below shows a large hysteresis between the heating and cooling curves.

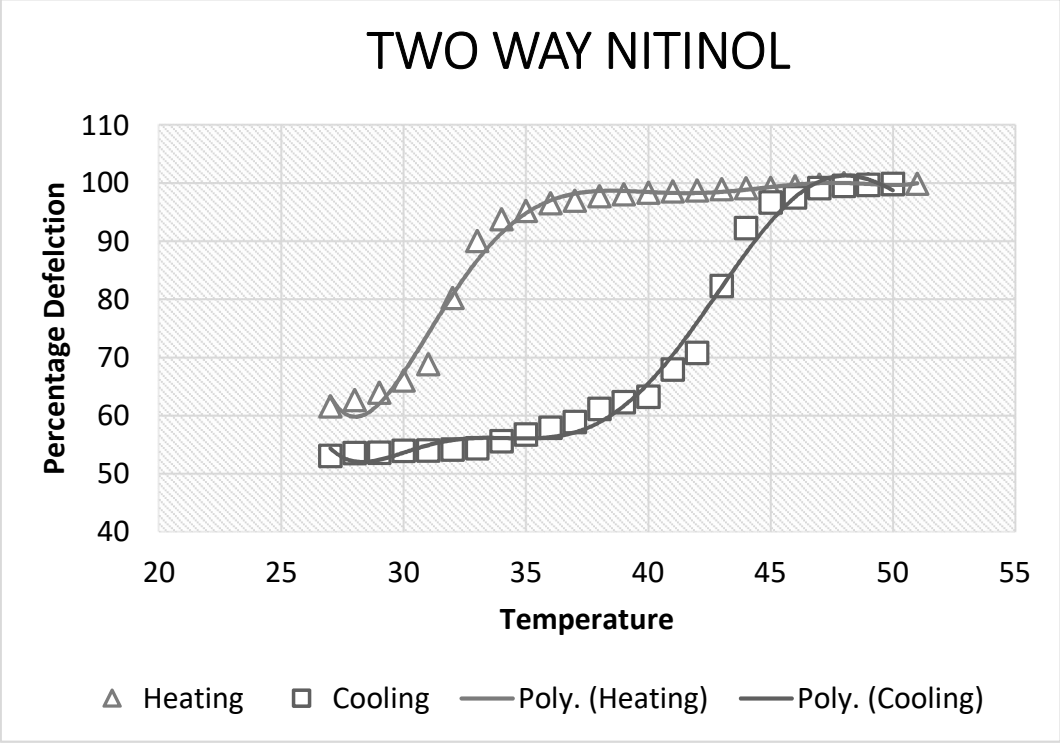

Graph 2-1 Two-way Nitinol Hysteresis loop

2.2.2. One-way Nitinol

One-way nitinol remembers only one unique shape. When Nitinol is in its low temperature state, it can be deformed owing to its low stiffness at this phase and will stay deformed until heated above its transition temperature [5]. Upon heating, it changes its shape back to its original shape. Experimental testing shows one-way nitinol has appreciably low hysteresis when compared to two-way nitinol. But one-way nitinol requires an external force to deform it at its low temperature martensite phase.

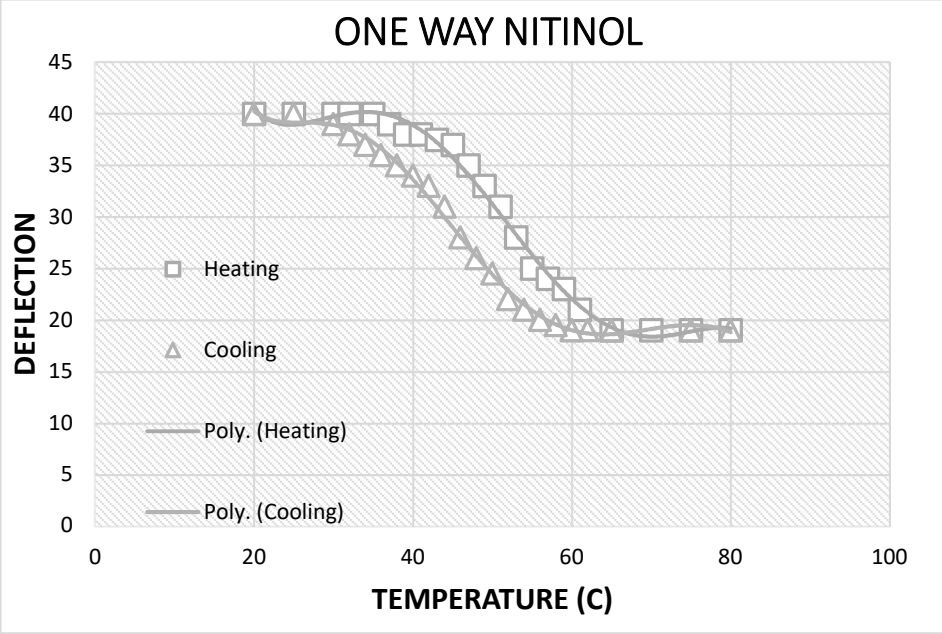

Graph 2-2 One-way Nitinol hysteresis loop

For effective functioning of the FCD and best dynamic response times, low hysteresis is essential. Hence one-way nitinol is preferred over two-way nitinol. To address the need for external loading to initially deform one-way nitinol, a novel dual spring setup is used. A helical nitinol spring is coupled with a stainless-steel tension spring. The force exerted by the tension spring can deflect the nitinol spring when it is in martensite form. Since the tension spring is

non-reactive to heat, with the increase in temperature, the tensile force generated by the nitinol spring becomes more than that of the stainless-steel spring.

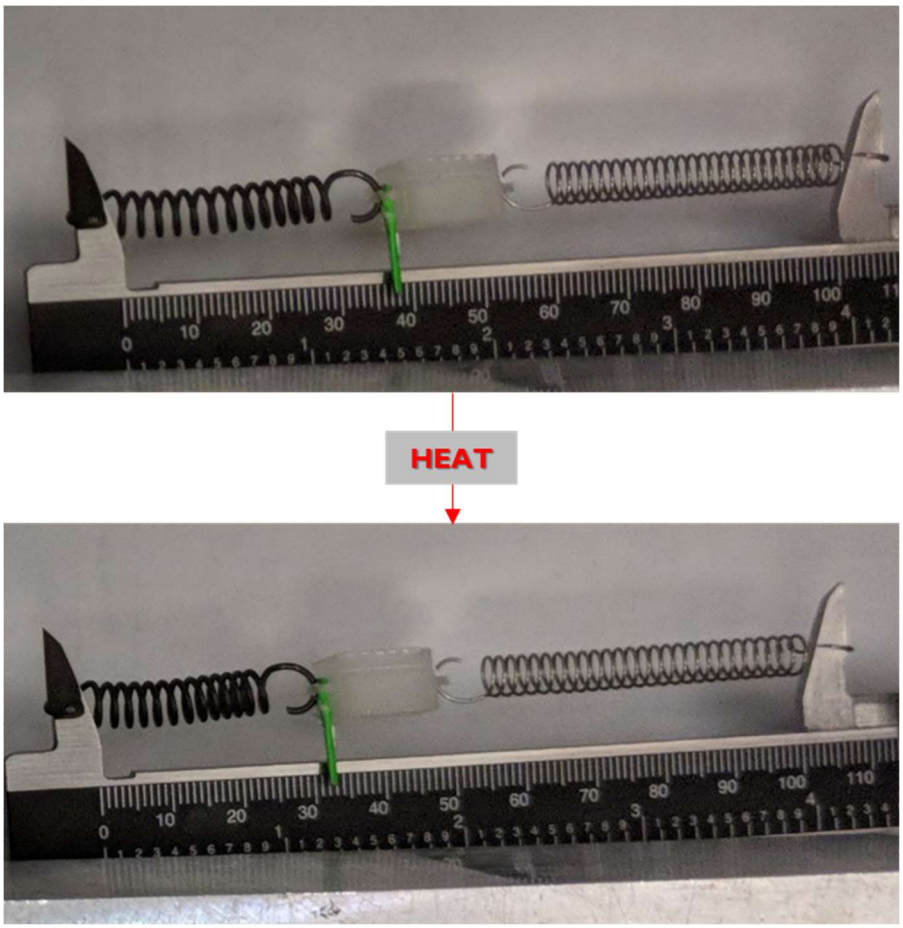

Figure 2-2 Nitinol helical spring phase change

2.3. Nitinol vs Bimetals

One alternative to using Nitinol as the actuator for the FCD was Bimetals. On studying the work documented by Ravi Teja Mutulaya [6] it is however clear to see that nitinol is superior when compared to bimetals in several ways. Nitinol produces much larger deflection than bimetals. Nitinol also produces considerably higher forces during phase change. This ensures that hydraulic pressure inside the flow control device does not interfere with the working of the

actuator. Large deflection per degree change in temperature is possible with Nitinol. Nitinol also occupies much lesser space to produce the same amount of deflection as nitinol.

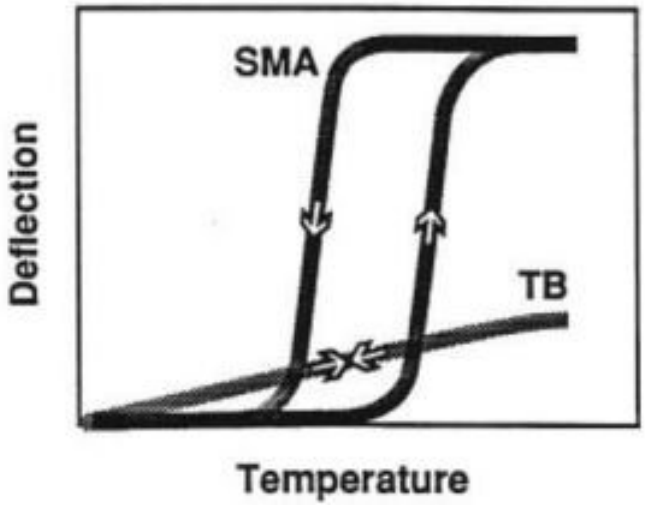

Figure 2-3 Shape memory alloy (SMA) vs Bimetal (TB)

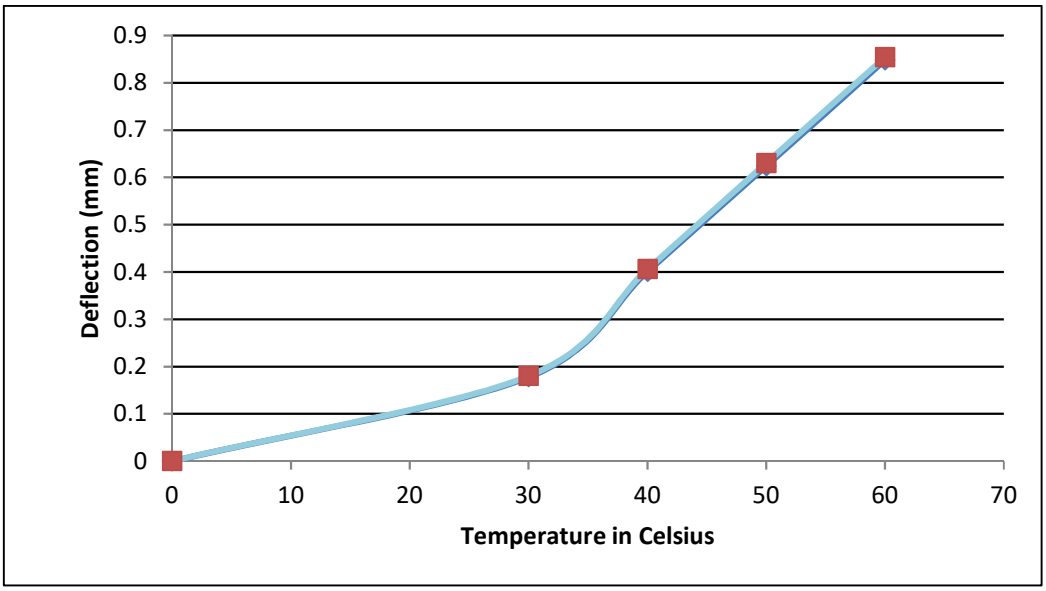

Graph 2-3 Bimetal deflection vs temperature [6]

Chapter 3

NITINOL CHARACTERIZATION

To design the heat sensitive actuator for the FCD it is essential to completely understand the behaviour of Nitinol helical springs. The main parameters of interest are:

- FORCE GENERATED AS A FUNCTION OF SPRING DIMENSIONS
- DISPLACEMENT AS A FUNCTION OF TEMPERATURE
- HYSTERESIS CURVES

To understand the behaviour of nitinol springs, an assortment of springs was experimentally tested. All springs are of the same standard temperature Nitinol, purchased from the same vendor.

Table 3-1 Inventory of nitinol springs tested

S. No	Mandrel Size (mm)	Wire Diameter(mm)	Spring length (mm)
1	4.75	0.25	15
2	4.75	0.25	25
3	4.75	0.25	35
4	4.75	0.5	15
5	4.75	0.5	25
6	4.75	0.5	35
7	4.75	1	15
8	4.75	1	25
9	4.75	1	35

It is to be noted that all the springs tested were one-way nitinol and hence all of them had to be coupled to a suitable stainless-steel spring to be tested. The experimental testing procedure of choice was performing thermal cycling on the dual spring system in a thermal chamber. A properly calibrated thermocouple was attached to the Nitinol spring to monitor its

temperature. As a preliminary test, thermal cycling of one arbitrary spring was done from 20°C to 80°C and back. This allowed for the overall hysteresis curve to be documented. The phase transition temperatures were also identified. As the nitinol spring in martensite phase is easily deformed, it is important to ensure that the deformation is purely due to the stainless-steel spring. To ensure that this is always the case, one or two thermal cycles are done for each spring combination before data is logged to ensure that the data obtained is accurate.

After preliminary testing, nitinol springs of various wire diameters and lengths were coupled with suitable stainless-steel springs, making sure that the stainless-steel spring is capable of producing ample deformation of the nitinol spring at room temperature. All stainless-steel springs used were standard springs of known dimensions and hence were used for force measurement as well (Formula listed below).

Equation 3-1 Force exerted on tension spring [7]

Equation: $T_F = I_T + (D \times k)$

Where:

T_F = Total Force exerted on spring

D = Distance spring is deflected

I_T= Initial tension force on spring

k = Spring constant determined by experiment or calculation

Displacement was another parameter that had to be documented. Image processing was used to measure exact the deflection produced by the nitinol spring. The total distance between the ends of both the springs was used as scale for displacement measurements because this value was always known and kept constant during the entire thermal cycling process.

In practical use cases of the FCD, the temperatures might not always be high enough to enable complete phase change of Nitinol to its Austenite phase. It is hence important to understand how nitinol behaves in the intermediate zone below its transition temperature. Experimental testing was done between various temperature ranges below the transition temperature of nitinol to better understand its behaviour in this region.

Chapter 4

FLOW CONTROL DEVICE DESIGN

The flow control device is responsible for housing the dual spring system. The springs are attached to a central block that is capable of altering flow rate. Design considerations are made to obtain optimum flow rates and pressure drops across the FCD. The flow control device has an inlet and outlet that allows fluid flow along the vertical direction, with the spring system located perpendicular to the path of fluid flow. The springs move a solid block across the inlet and outlet orifice, thereby varying the hydraulic diameter of the flow. Since it is necessary for the nitinol spring to be contact with the fluid, the inlet hydraulic diameter is made bigger than the outlet hydraulic diameter, ensuring that fluid fills up the horizontal housing that contains the dual spring system. The horizontal housing also has groves on all four sides. The grooves have two purposes: to reduce friction between the moving block and the walls, and to provide a non-zero fluid delivery from the FCD even when the block completely seals the exit.

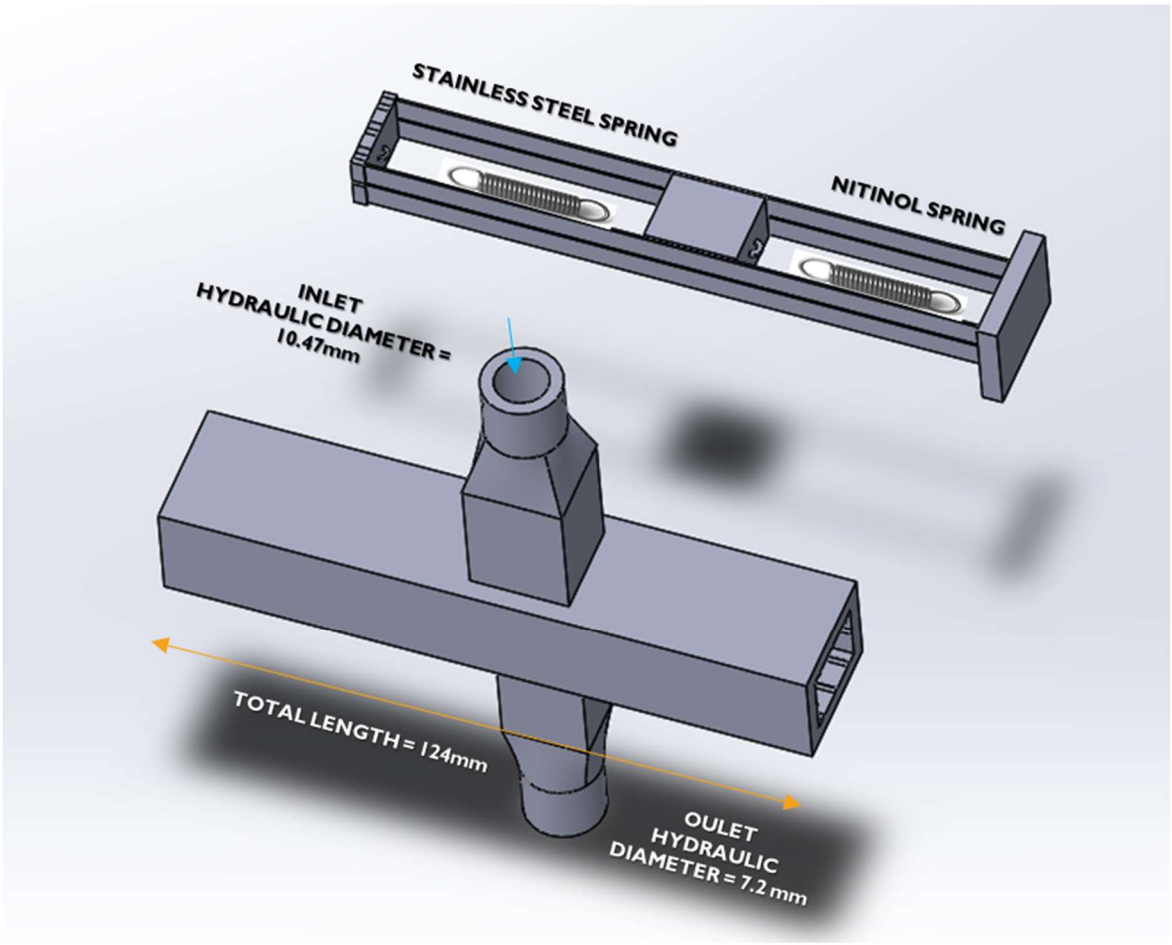

Figure 4-1 FCD design

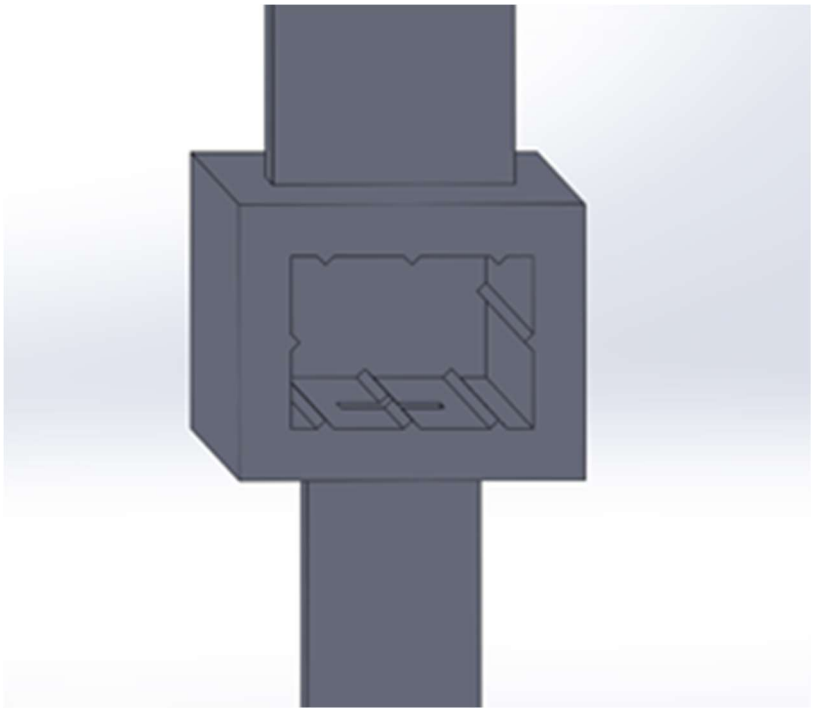

Figure 4-2 FCD groves and rectangular cross section

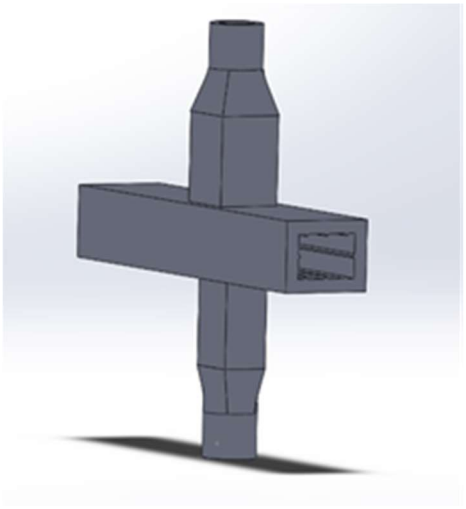

Figure 4-3 FCD side view

The flow control device has rectangular cross sections throughout its flow regions. This helps ensure linear change in hydraulic diameter with movement of the block. Experimental and CFD testing on the FCD was performed to validate linear change in flow rate with the change in block position.

Chapter 5

FLOW CONTROL DEVICE PROTOTYPE TESTING

The flow control device prototype was manufactured using 3D printing. The prototype consists of three individual components: The external housing, a holder and the block. The springs are loaded onto the holder with the block in the middle and then slid into the main housing. The holder is then sealed using a leak proof sealant. Photographs of the prototype are provided in the appendix.

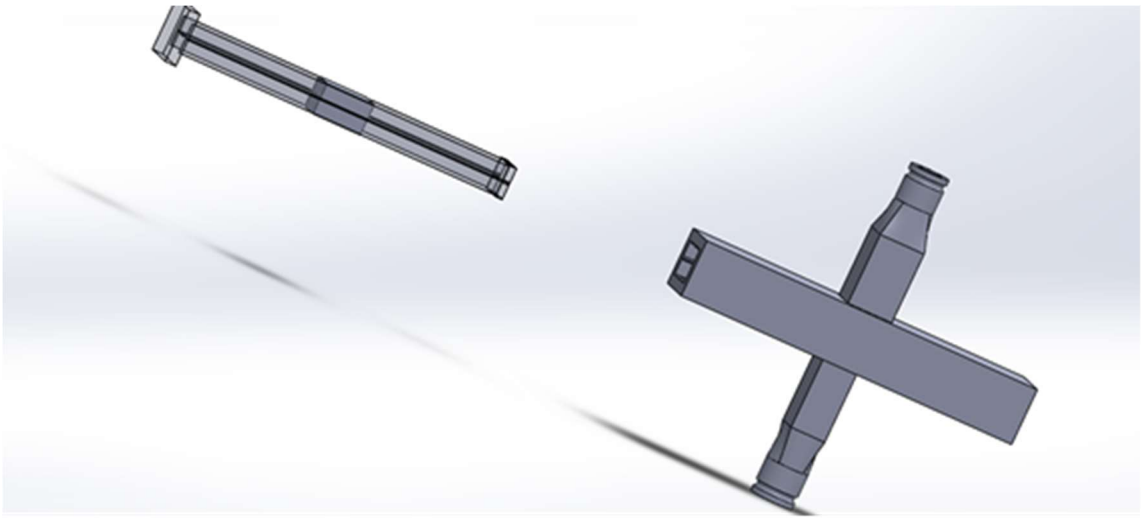

Figure 5-1 FCD assembly

5.1. Experimental test rig

An experimental test rig is used to analyse the performance of the FCD. A heat exchanger is used to control the temperature of the coolant being delivered to the FCD. The test rig is populated with flow, pressure and temperature sensors at various points on the circuit. A relief valve is connected in parallel to the FCD to allow for optimum pressure drop across the FCD. Data acquisition devices are used to log data from the various sensors. Flow rate changes for change in coolant temperature is recorded and documented.

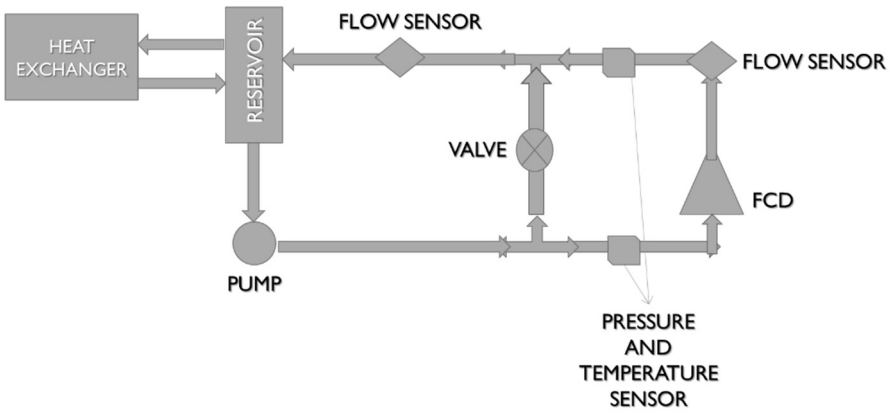

Figure 5-2 Test rig schematic

The pump used is a Swiftech MCP50X pump which has pulse width modulated (PWM) control to modify flow rate delivery. The pump is a centrifugal pump with a range between 1200 to 4500 rpm.

Figure 5-3 Swiftech MCP50X pump [8]

The pressure sensors of choice were the Honeywell MLH050PGL06E silicon Piezo-resistive pressure sensors.

Figure 5-4 Honeywell MHL series pressure sensor [9]

The Omega FTB 421 flowmeter was selected as it has range of operation from 0.1 to 2.5 LPM. It has accuracy of ± 3% of reading normal range and repeatability of 0.5% FS normal range.

Figure 5-5 Omega FTB421 Flowmeter [10]

Thermocouple probes from OMEGA are used. The T-type thermocouple with glass filled nylon connector is rated for temperatures up to 220°C.

Figure 5-6 Thermocouple probe [10]

A data acquisition unit is used to log data from the various sensors. Included companion software is used to set intervals of data logging.

Figure 5-7 Data acquisition unit

Chapter 6

RESULTS

6.1. CHARACTERIZATION OF NITINOL HELICAL SPRINGS

Force as a function of spring dimensions is plotted from data recorded by experimental testing. The dual spring setup is placed in a thermal chamber where thermal cycling is done. Note that only heating cycles are plotted below.

Nitinol springs of various wire diameters and lengths are coupled with suitable stainless-steel springs, making sure that the stainless-steel spring is capable of producing ample deformation of the nitinol spring at room temperature. The stainless-steel springs used are all standard springs of known dimensions and hence they can be used for force measurement as well. The forces observed in plots 6-1 and 6-2 show sums of structural as well as phase transformation forces.

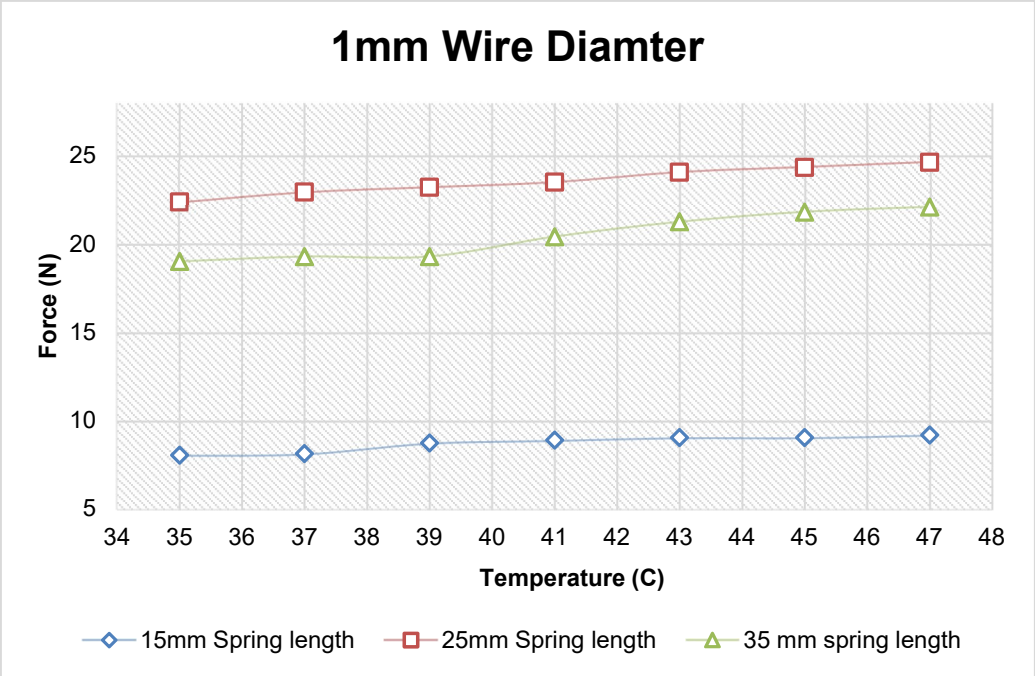

Graph 6-1 Aggregate structural and phase change force for 1mm Nitinol spring

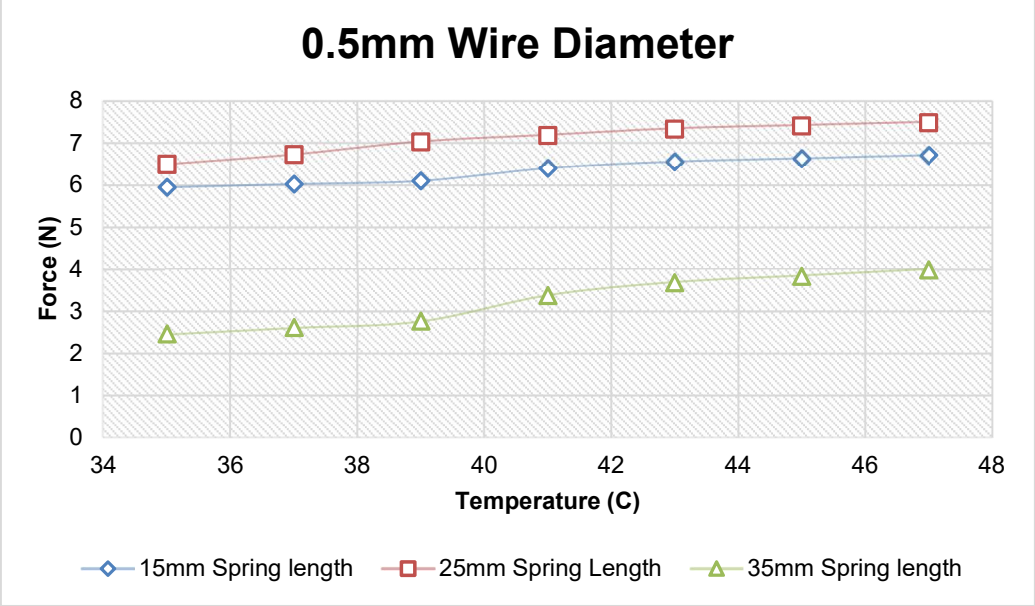

Graph 6-2 Aggregate structural and phase change force for 0.5mm Nitinol spring

Graph 6-3 has nine individual data points that provide force generated due to phase change for nine unique nitinol springs of different dimensions. From the plot it is clear to see that the springs with larger wire diameters and solid spring lengths are able to generate more force when compared to springs with smaller wire diameters and solid spring lengths. The forces plotted are purely due to phase change and do not include structural resistance.

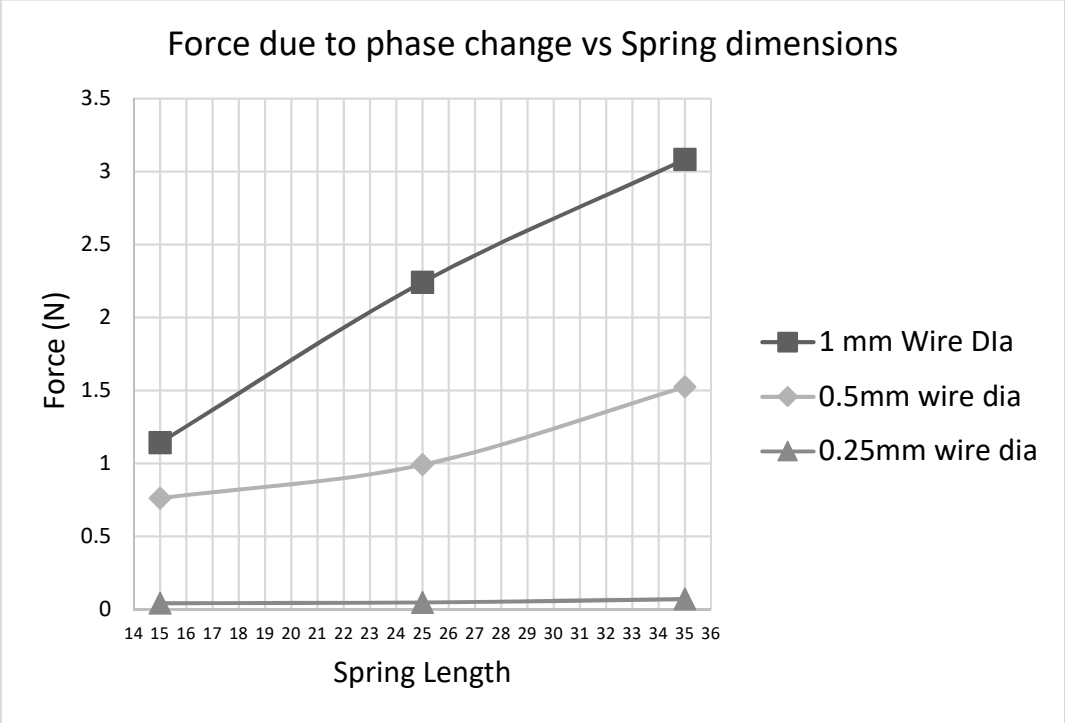

Graph 6-3 Force generated by nitinol helical springs due to phase change

Displacement generated by Nitinol as a function of temperature of Nitinol is plotted in the graph below. This plot corresponds to one combination of Nitinol and stainless-steel spring. Thermal cycling for numerous other spring combinations were also done in the thermal chamber to identify the combination that would provide the highest displacements for the temperature range in which the FCD would function. The best combination is for acceptable

total separation is tabulated below. The plot provided corresponds to the same spring combination.

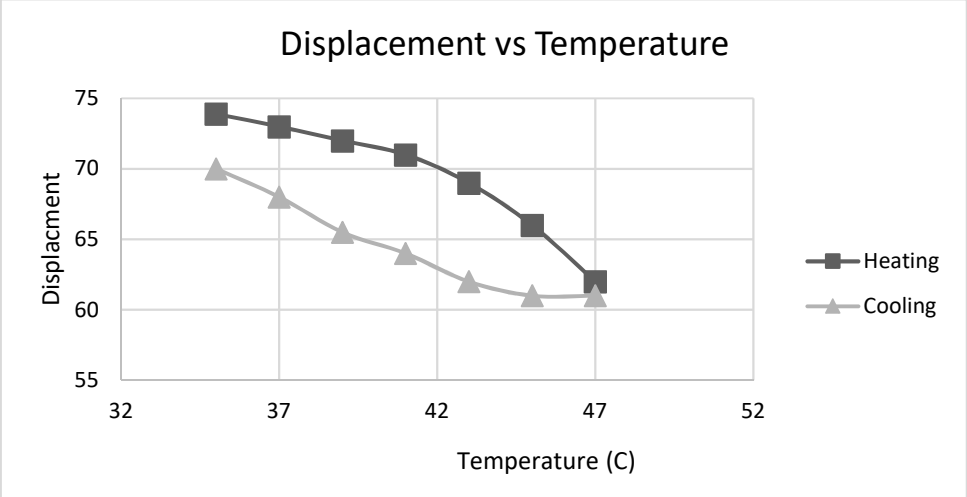

Graph 6-4 Displacement characterization of Nitinol helical springs

Table 6-1 Selected Nitinol Stainless steel spring combination

NITINOL SPRING	STAINLESS STEEL SPRING
• 1mm Wire diameter • 25mm Spring length • 4.75mm mandrel size DEFELECTION ACHIEVED FOR 140mm SEPARATION, 35°C to 47°C = **13mm**	• OD (in) 0.240 • Length (in) 1.130 • Rate (lbs/in) 0.870 • Initial Tension (lbs) 0.200 • Sugg. Max. Defl. (in) 1.600 • Sugg. Max. Load (lbs) 1.600 • Wire Dia. (in) 0.022 • Material Stainless Steel • Finish None

Hysteresis loops for temperature ranges that do not span the entire transition temperature ranges are plotted below after experimental testing. It is clear to see that hysteresis still exists even if transition temperature is not attained.

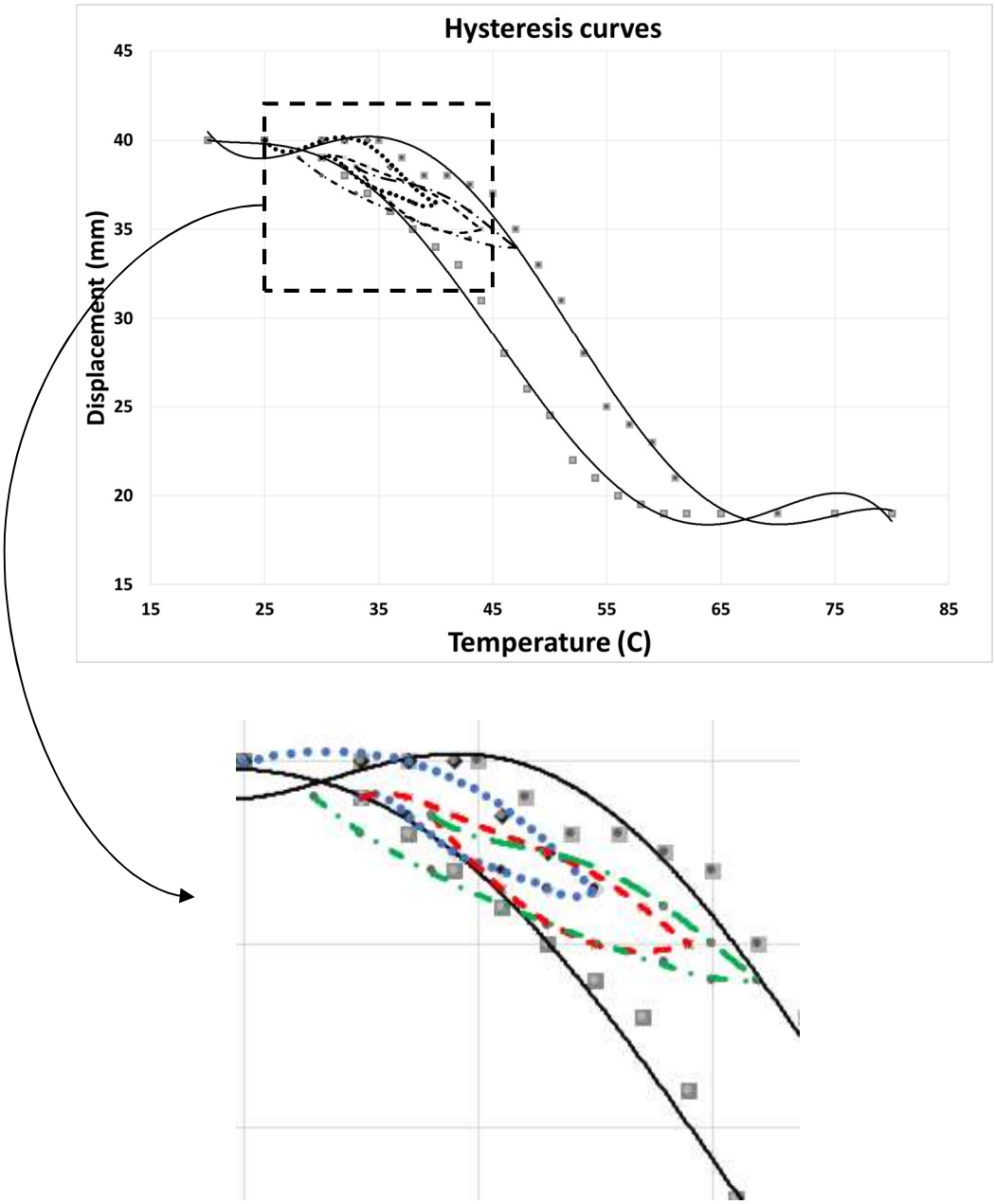

Graph 6-5 Nitinol hysteresis characterization

6.2. FCD CFD ANALYSIS

CFD analysis was done on the FCD to analyse the fluid flow rate for various position of the block. Linear change in flow rate is important to ensure that there are no sudden changes in flow rate with change in block position [11]. Change in block position effectively reduces the hydraulic diameter of the outlet. The plot below shows fairly linear change in flow rate with change in block position.

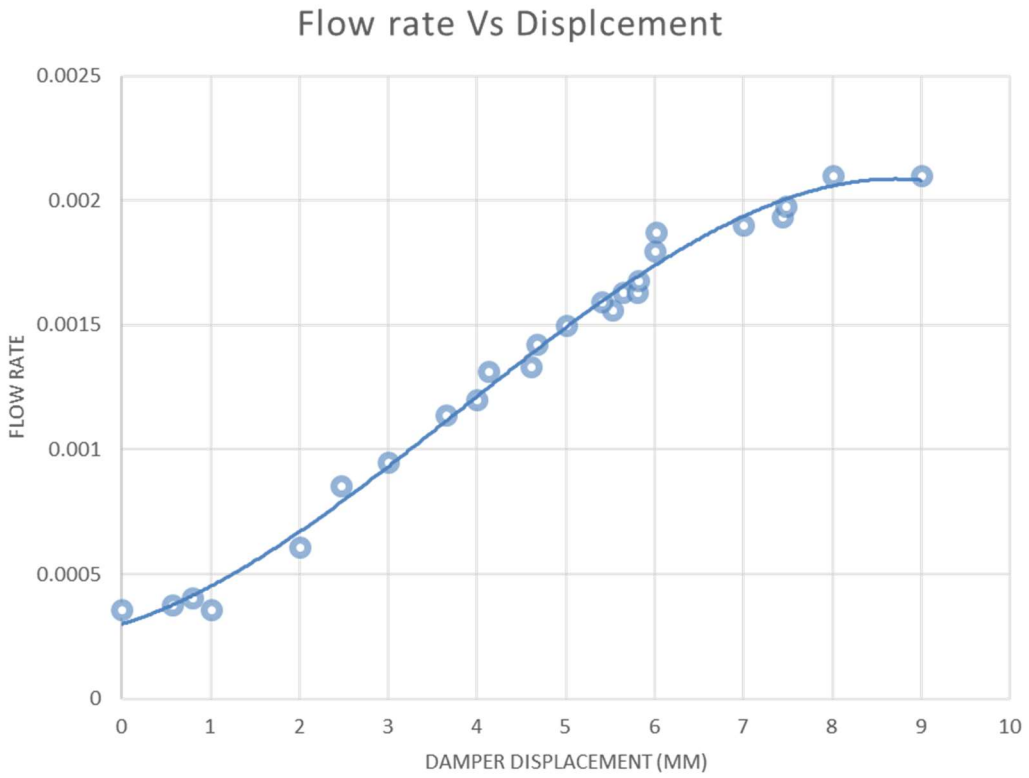

Graph 6-6 CFD results of FCD

6.3. FCD PROTOTYPE EXPERIMENTAL TEST

The experimental test rig explained in section 5.1 is used to quantify the performance of the FCD prototype. Data acquisition from the various sensors in the test rig was done for every three seconds. Constant flow rate was provided throughout the experiment by the

pump. Temperature of the water was varied using the heat exchanger. From the experimental data obtained, a flow rate change of about 0.1 lpm was observed for a temperature change from 20°C to 45°C. The change in flow rate is fairly linear with respect to temperature.

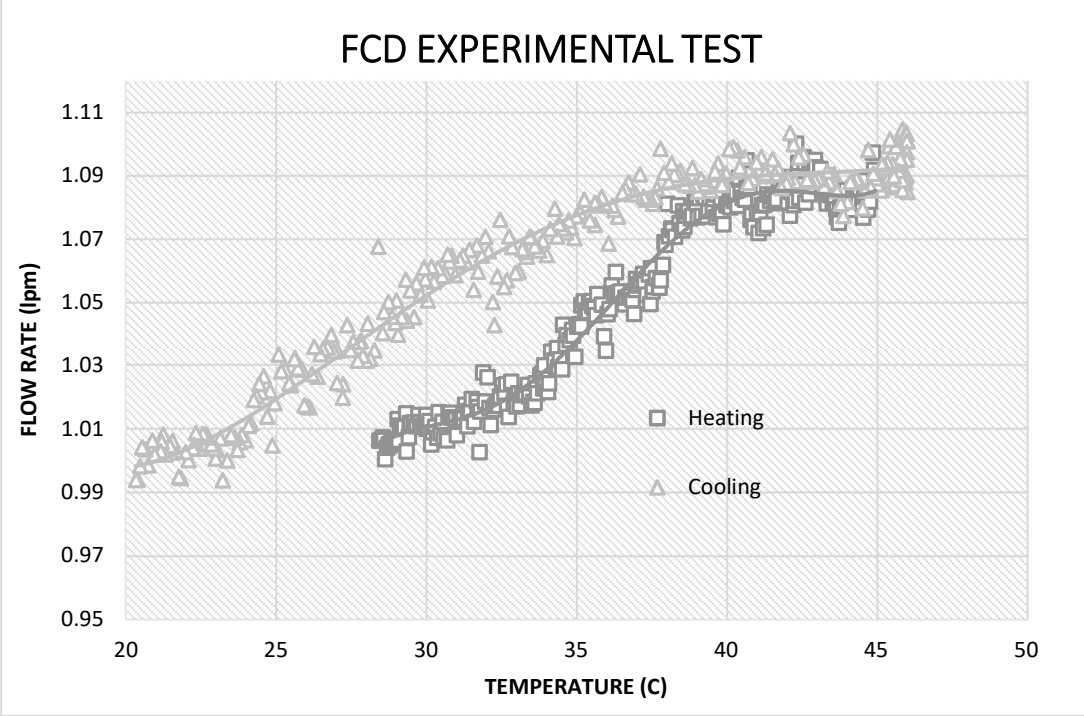

Graph 6-7 Experimental results of FCD

Conclusion

From detailed experimental study it is observed that one-way nitinol is better than two-way nitinol owing to lower hysteresis. The novel dual spring setup allows for one-way nitinol to be mechanically loaded at room temperature. From extensive experimentation on Nitinol springs to estimate force during phase change and displacement characteristics optimum spring selection was possible.FCD was designed to vary flow rates based on required temperature difference. The FCD prototype was able to produce 0.1 lpm change in flow rate when operated between 25°C and 45°C.

Future Work

Future work primarily involves miniaturizing the FCD. Comprehensive characterisation of nitinol torsion springs needs to be done to aid in miniaturizing the FCD. Higher precision manufacturing methods can be used to provide better results. Friction can be reduced by using different materials in the manufacturing process. Low temperature nitinol can also be tested for use in less power dense scenarios with lower temperature values.

Chapter 7

APPENDIX

Supplementary Pictures

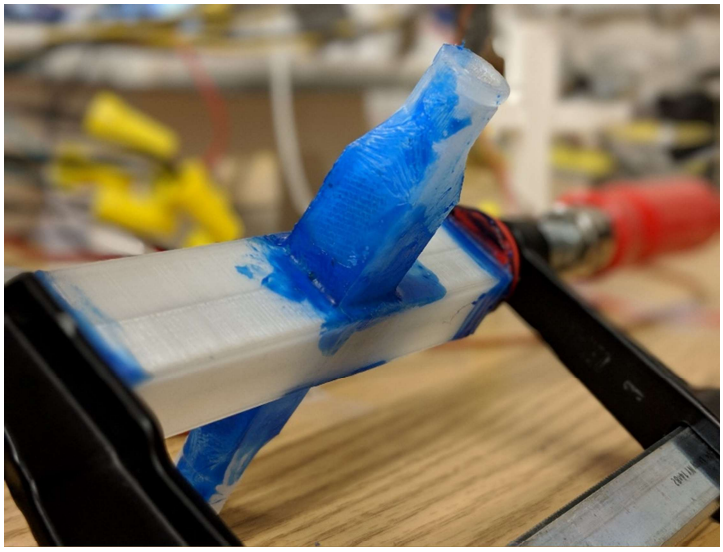

Figure 7-1 FCD prototype

Figure 7-2 Water sealed FCD prototype

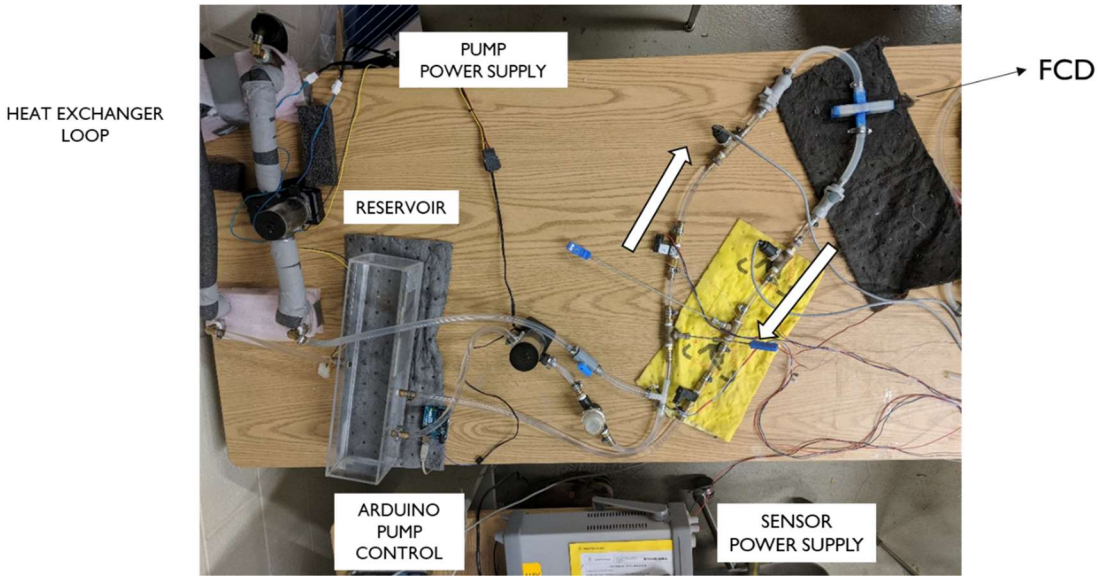

Figure 7-3 Test Rig

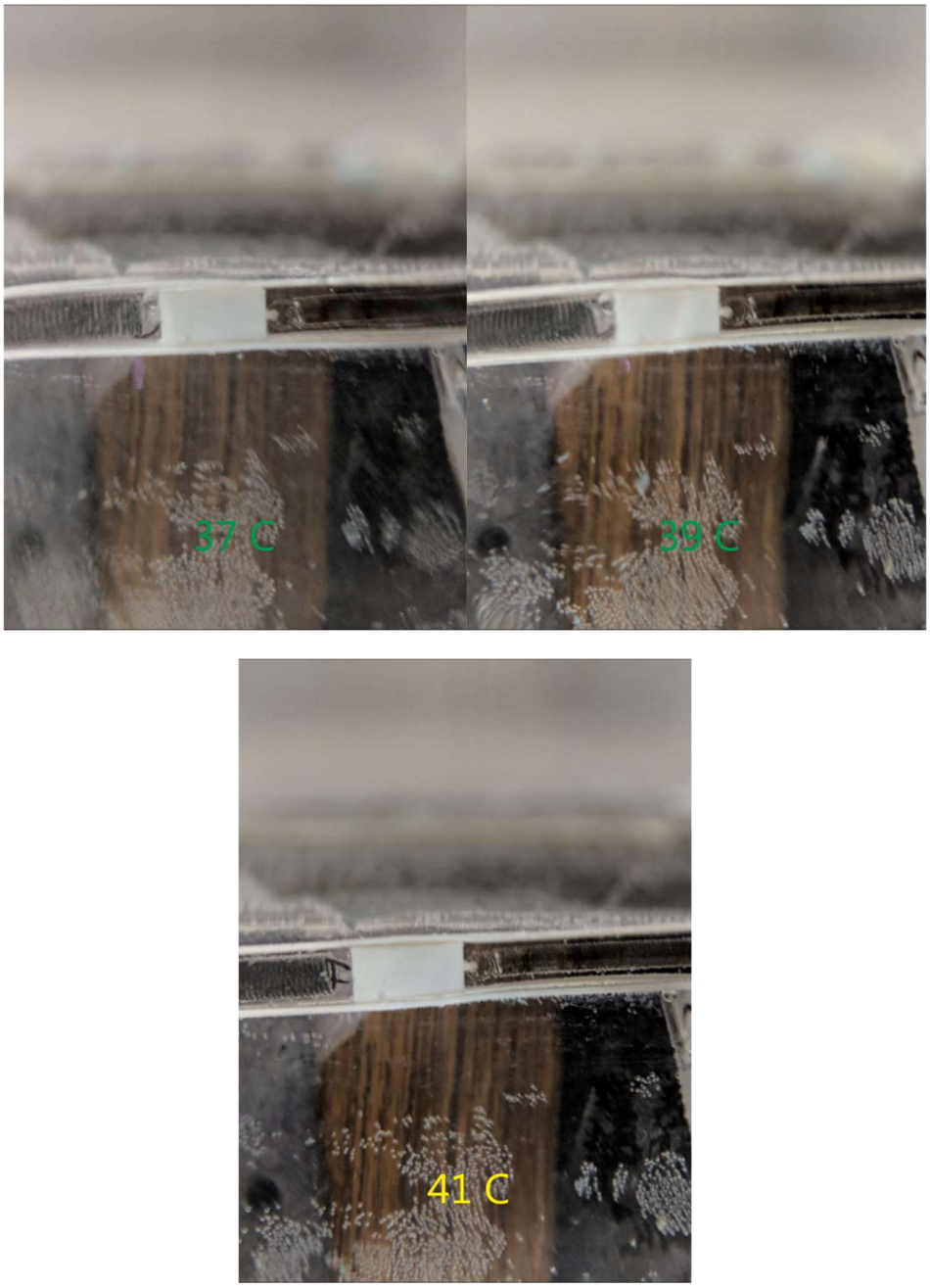

Figure 7-4 Dual Spring System underwater tests (a)

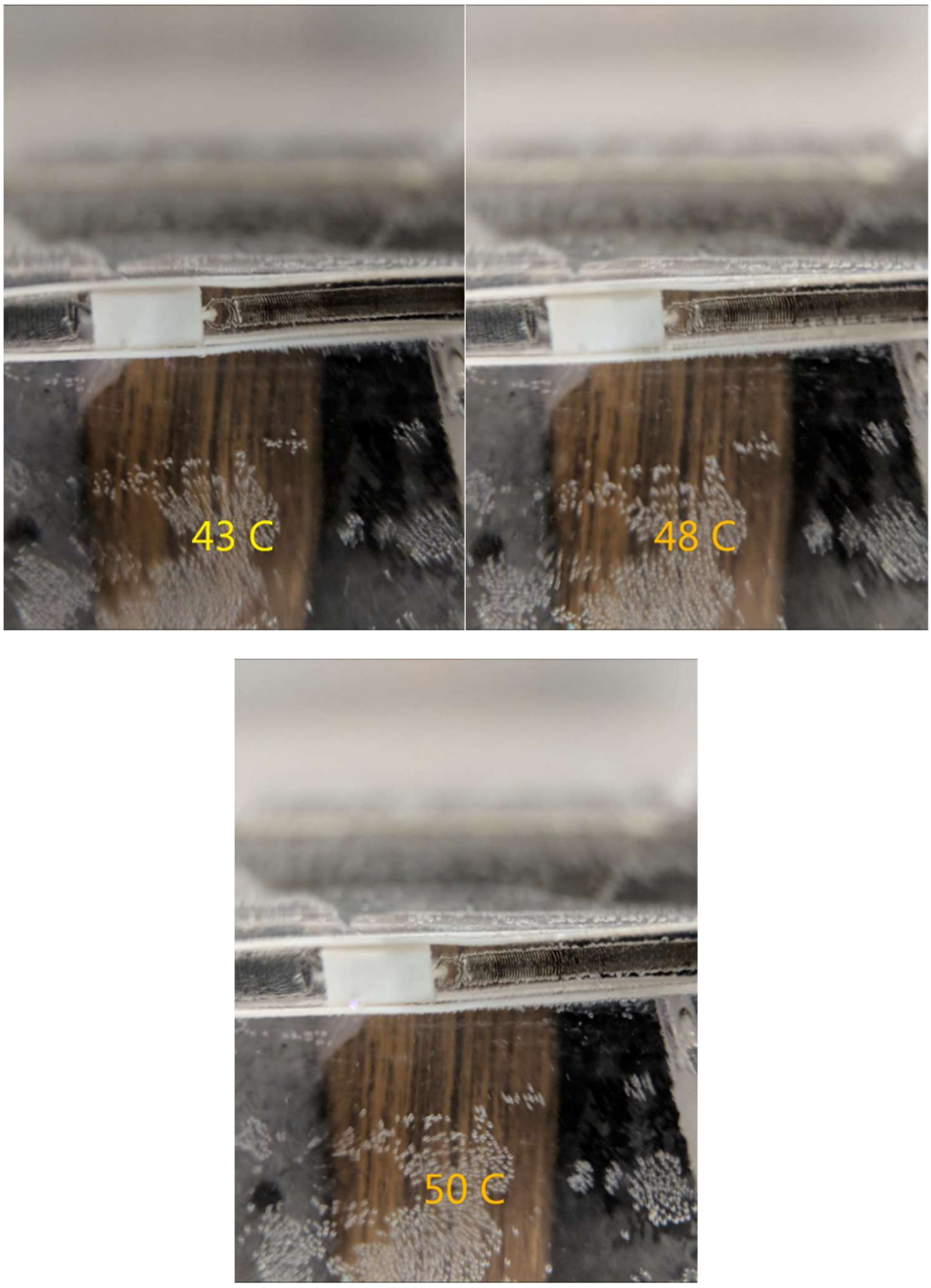

Figure 7-5 Dual Spring System underwater tests (b)

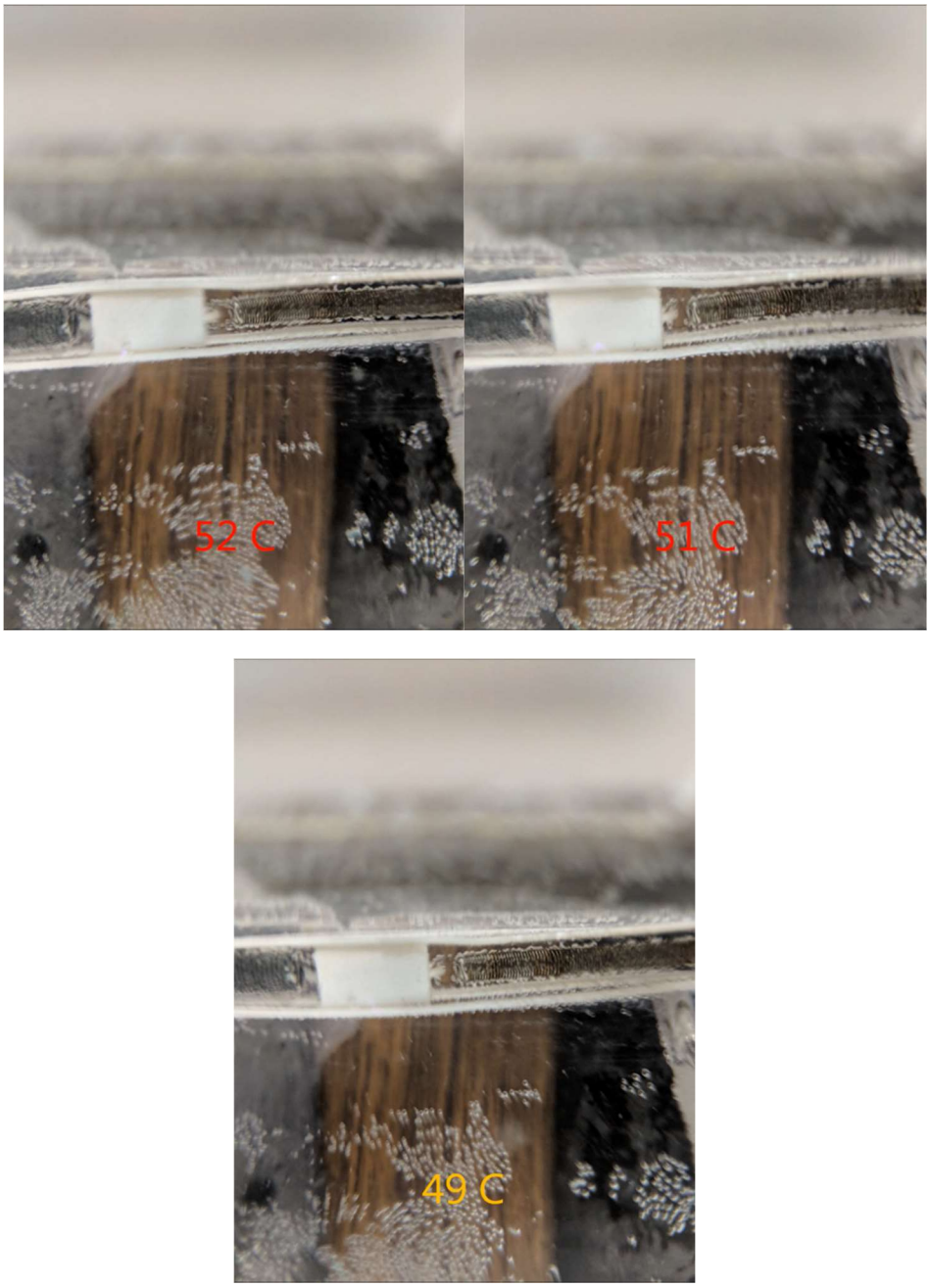

Figure 7-6 Dual Spring System underwater tests (c)

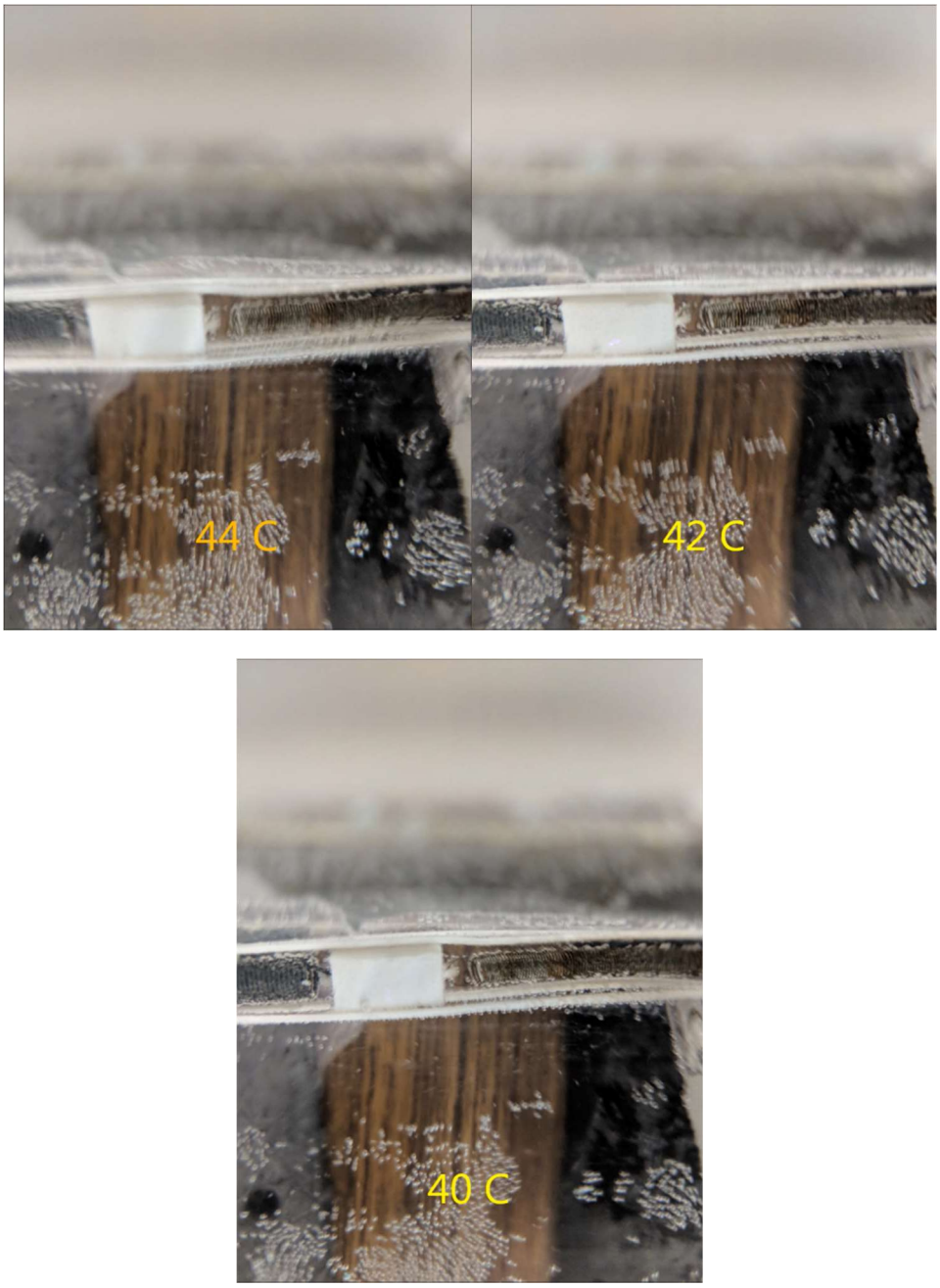

Figure 7-7 Dual Spring System underwater tests (d)

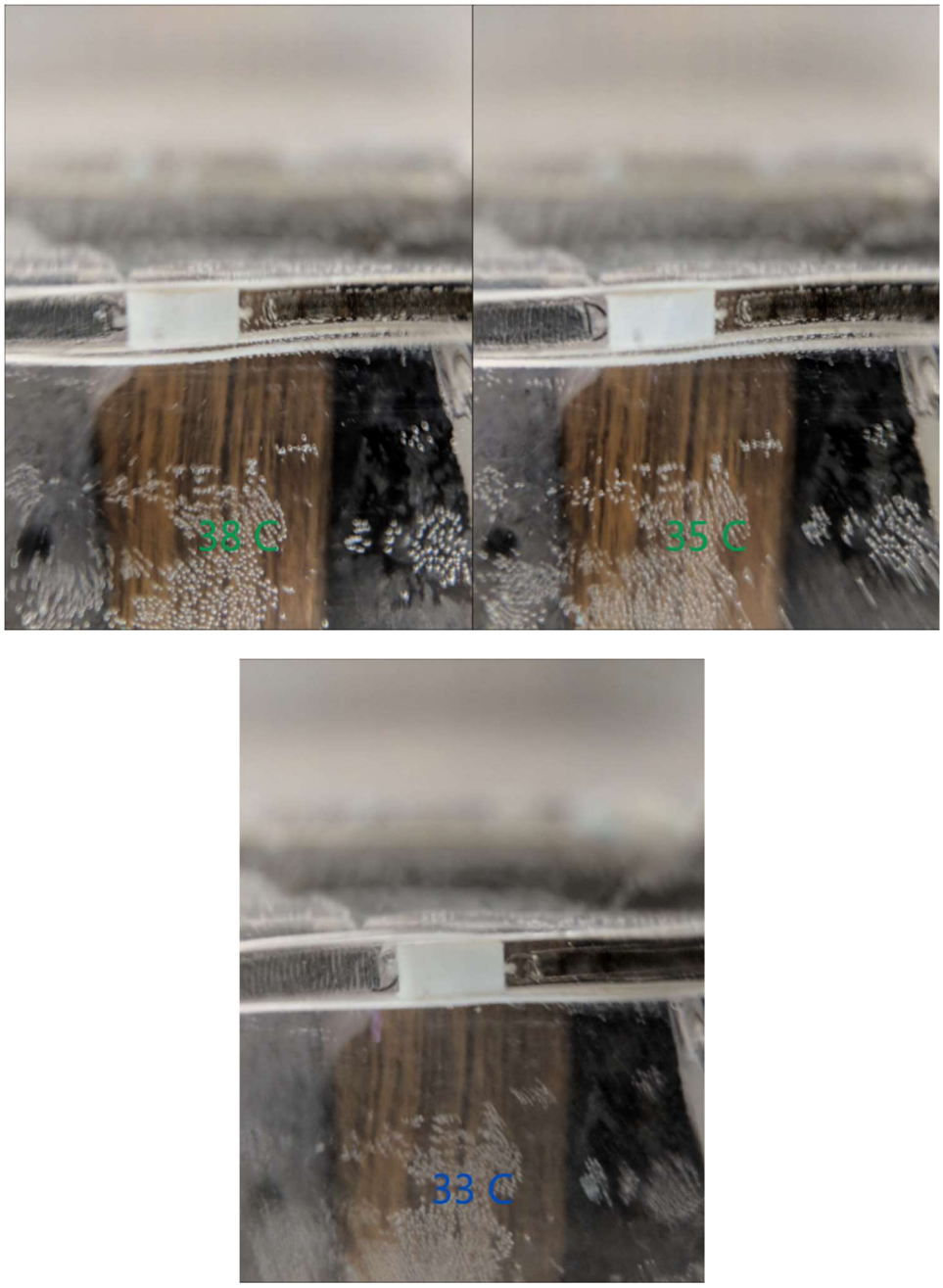

Figure 7-8 Dual Spring System underwater tests (e)

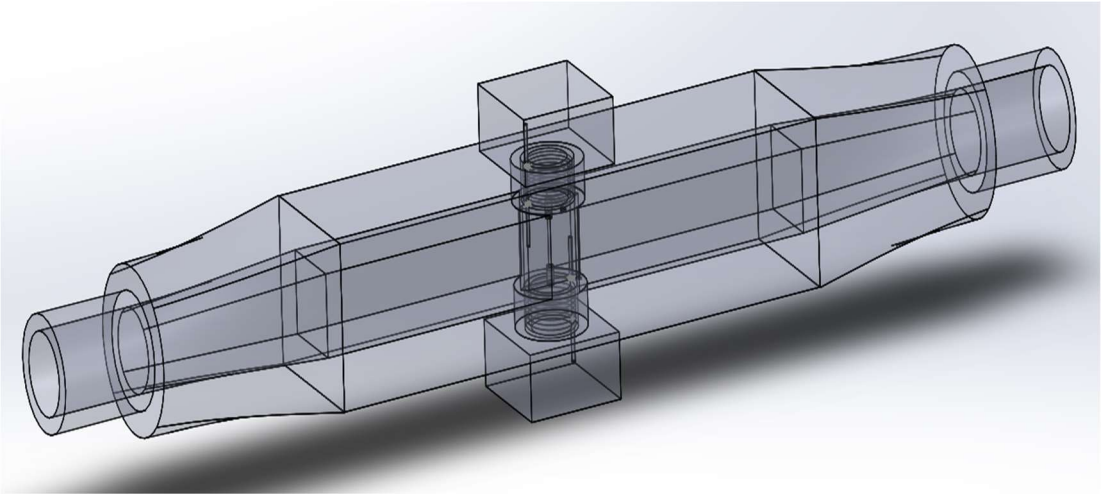

Figure 7-9 Future work: Torsion spring FCD design suggestion (a)

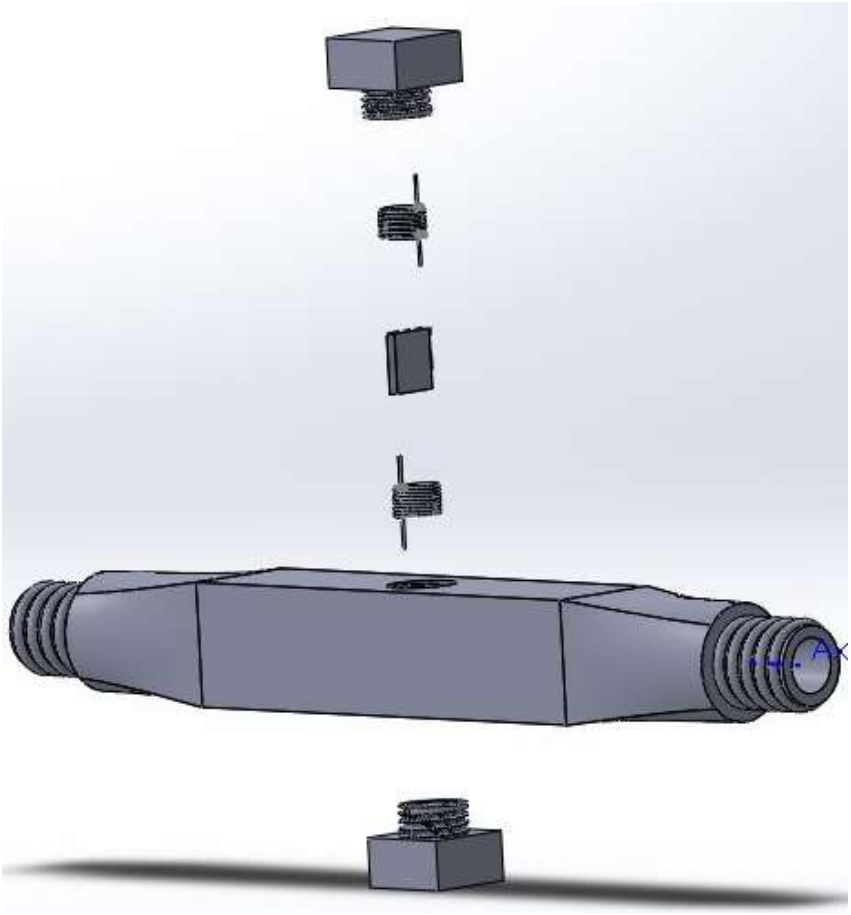

Figure 7-10 Future work: Torsion spring FCD design suggestion (b)

References

[1] R. Mahajan, C.-P. Chiu and G. Chrysler, “Cooling a microprocessor chip,” *Proceedings of the IEEE,* pp. vol. 94, no. 8, pp. 1476-1486, 2006.

[2] K. A. Shah, “Design of an Improved Flow Control Device for Dynamic Cold Plates,” 2016.

[3] M. Sahini, C. Kshirsagar, M. Kumar, D. Agonafer, J. Fernandes, J. Na, V. Mulay, P. McGinn and M. Soares, “Rack-level study of hybrid cooled servers using warm water cooling for distributed vs. centralized pumping systems,” in *Thermal Measurement, Modeling & Management Symposium (SEMI-THERM), 2017 33rd*, 2017/3/13.

[4] “http://jmmedical.com/resources/221/Nitinol-Technical-Properties.html,” [Online].

[5] P. F. Auricchio, “One Way and Two Way–Shape”.

[6] R. T. Mutulaya, “Thesis - controlling flow using bimetallic strips,” University of Texas at Arlington. .

[7] “https://www.engineersedge.com/spring_extension_calc.htm,” [Online].

[8] “http://www.swiftech.com/,” [Online].

[9] “http://www.digikey.com/product-detail/en/MLH050PGL06E/480-5408-ND/3306012,” [Online].

[10] “http://www.omega.com/,” [Online].

[11] R. Kasukurthy, P. S. Challa, R. R. Palanikumar, B. R. Manimaran and D. Agonafer, “Flow Analysis and Linearization of Rectangular Butterfly Valve Flow Control Device for Liquid Cooling,” *IEEE itherm,* 2018.

Biographical Information

Rishi Ruben Palanikumar received his bachelor's degree (BE) in Mechanical Engineering from Anna University in 2016. In August 2016, he began his graduate studies at the University of Texas at Arlington. Rishi Ruben Palanikumar joined the EMNSPC to conduct research on dynamic cold plates for multi-chip modules. Rishi Ruben Palanikumar received his MS degree in Mechanical Engineering from the University of Texas at Arlington in May 2018.